# Polycyclic Aromatic Hydrocarbons of Asphaltenes Analyzed by Molecular Orbital Calculations with Optical Spectroscopy

**ARTICLE** *in* ENERGY & FUELS · DECEMBER 2006

Impact Factor: 2.79 · DOI: 10.1021/ef060250m

# Polycyclic Aromatic Hydrocarbons of Asphaltenes Analyzed by Molecular Orbital Calculations with Optical Spectroscopy

Yosadara Ruiz-Morales*,† and Oliver C. Mullins‡

*Programa de Ingeniería Molecular, Instituto Mexicano del Petróleo, Eje Central Lázaro Cárdenas 152, México D.F. 07730, México, and Schlumberger−Doll Research, Ridgefield, Connecticut 06877*

*Received June 1, 2006. Revised Manuscript Received October 15, 2006*

The number and geometry of the rings in polycyclic aromatic hydrocarbons (PAHs) in petroleum asphaltene has remained unresolved for many years. Many sophisticated imaging and spectroscopic methods have been utilized to narrow the list of candidate structures for asphaltene PAHs. Here, we exploit a canonical property of petroleum asphaltenes, their color, along with their fluorescence emission properties. These universal spectral properties are analyzed through the lens of molecular orbital (MO) calculations, thereby providing quantitative bounds on asphaltene PAH systems. Energetic considerations mandate that these fused aromatic ring systems are predominantly aromatic sextet carbon (within the Clar representation) but not entirely sextet carbon. Matching the ubiquitous asphaltene spectral data with MO calculations shows that asphaltene ring systems predominantly consist of 4−10 rings. PAHs with 6−8 rings are most predominant in petroleum asphaltenes. Not surprisingly, polydispersity is implied in this analysis. These results are very consistent with all direct imaging of asphaltene PAHs. When these results are coupled with known molecular weights of asphaltenes, we find that asphaltene molecules possess primarily one fused ring system per molecule. This finding is independently obtained when combining MO results with spectral dispersion measured for asphaltene diffusion constants. The monomeric molecular structure of asphaltenes is supported, and the archipelago model is refuted.

## 1. Introduction

The importance of asphaltenes continues to grow for a variety of purposes. Heavy oils and unconventional hydrocarbon resources rich in asphaltene are increasingly being exploited to sate the increasing thirst for petroleum around the world.[1] Increases in efficiency for both production and refining of petroleum are mandated by the increasing complexities associated with ever far-reaching hydrocarbon utilization. For example, limits are continually being pushed in deepwater production of crude oil. Understanding compartmentalization of reservoir flow units in such high-cost settings is being revealed by new analytical chemistry methods.[2] In a broader context, predicting the properties of crude oils requires understanding their constituents. Petroleomics, the determination of structure−function relations in crude oil, is built on the foundation of establishing the petroleome, the complete listing of all components in a crude oil.[1] Within this framework, it is essential to understand asphaltene molecular structure.

Asphaltene molecular weight has been a controversy for many years, but this issue is finally being resolved. Boduszynski used field ionization mass spectrometry (FIMS) to obtain an average asphaltene molecular weight of ∼800 g/mol (Da).[3] Groenzin et al. obtained nearly the same results by measuring asphaltene molecular diffusion at a low concentration (6 mg/L in toluene) using time-resolved fluorescence depolarization (TRFD).[4−6] Subsequently, all mass spectral techniques support these findings, including electrospray ionization Fourier transformation, ion cyclotron resonance mass spectromemtry (ESI−FT-ICR−MS),[7] atmospheric pressure photoionization (APPI),[8] and atmospheric pressure chemical ionization (APCI).[8,9] It has recently been shown that laser desorption ionization mass spectrometry (LDI−MS), subsuming laser desorption mass spectrometry (LDMS), and matrix-assisted laser desorption ionization (MALDI) is also consistent with all other mass spectral methods when applied to asphaltenes.[10] It is now understood that excess laser power and an excess concentration of asphaltene yield LDI−MS results that greatly exceed the actual asphaltene molecular weight.[10]

* To whom correspondence should be addressed. Telephone: +(5255) 9175-8180. Fax: +(5255) 9175-6380. E-mail: yruiz@imp.mx.

† Instituto Mexicano del Petróleo.

‡ Schlumberger−Doll Research.

(1) Mullins, O. C., Sheu, E. Y., Hammami, A., Marshall, A. G., Eds. *Asphaltenes, Heavy Oils, and Petroleomics*; Springer: New York, 2007.

(2) Mullins, O. C.; Rodgers, R. P.; Weinheber, P.; Klein, G. C.; Venkatramanan, L.; Andrews, B.; Marshall, A. G. Oil reservoir characterization via crude oil analysis by downhole fluid analysis in oil wells with visible−NIR spectroscopy and by laboratory analysis with ESI−FT-ICR−mass spectroscopy. *Energy Fuels*, **2006**, *20*, 2448−2456.

(3) Boduszynski, M. M. In *Chemistry of Asphaltenes*; Bunger, J. W., Li, N. C., Eds.; American Chemical Society: Washington, D.C., 1984, Chapter 7.

(4) Groenzin, H.; Mullins, O. C. Asphaltene molecular size and structure. *J. Phys. Chem. A* **1999**, *103*, 11237.

(5) Groenzin, H.; Mullins, O. C. Molecular sizes of asphaltenes from different origin. *Energy Fuels* **2000**, *14*, 677.

(6) Groenzin, H.; Mullins, O. C. Asphaltene molecular size and weight by time-resolved fluorescence depolarization. In *Asphaltenes, Heavy Oils, and Petroleomics*; Mullins, O. C., Sheu, E. Y., Hammami, A., Marshall, A. G., Eds.; Springer: New York; Chapter 2, 2007.

(7) Rodgers, R. P.; Marshall, A. G. Petroleomics: Advanced characterization of petroleum derived materials by Fourier transform ion cyclotron resonance mass spectrometry (FT-ICR MS). In *Asphaltenes, Heavy Oils, and Petroleomics*; Mullins, O. C., Sheu, E. Y., Hammami, A., Marshall, A. G., Eds.; Springer: New York; Chapter 3, 2007.

(8) Merdrignac, I.; Desmazieres, B.; Terrier, P.; Delobel, A.; Laprevote, O. Analysis of raw and hydrotreated asphaltenes using off-line and on-line SEC/MS coupling. Proceedings−Heavy Organic Deposit, Los Cabos, Mexico, 2004.

(9) Cunico, R. I.; Sheu, E. Y.; Mullins, O. C. Molecular weight measurement of UG8 asphaltene by APCI mass spectroscopy. *Pet. Sci. Technol.* **2004**, *22*, 787−798.

10.1021/ef060250m CCC: $37.00 
Published on Web 12/21/2006

In addition to TRFD results on asphaltene molecular diffusion, there are now three other diffusion measurements of asphaltenes. Taylor dispersion (TD) utilizing optical absorption is in exact agreement with the TRFD results on the same sample.[11] Fluorescence correlation spectroscopy (FCS) has been used to measure translational diffusion constants of both petroleum[12] and coal asphaltenes[12,13] and obtains results in close agreement with TRFD results. Nuclear magnetic resonance (NMR) has also been used to measure translation diffusion constants of asphaltene molecules.[14] The results are close to but slightly higher than the other diffusion methods; however, the lowest concentrations used for the NMR studies (because of signal-to-noise issues) were comparable to concentrations of dimer formation.[15] Thus, all diffusion measurements are in agreement with all mass spectral techniques. Asphaltene molecular weights are roughly 750 Da, with a full width at half-maximum (fwhm) of 500−1000 Da and a high mass tail. Now that the centroid of the asphaltene molecular weight is established, it is likely that there will be significant focus on the high mass tail.

In addition, measurements that had given artificially high asphaltene molecular weight are now understood to suffer from limitations. For example, vapor pressure osmometry (VPO) on asphaltenes is performed at concentrations that are too high to necessarily avoid asphaltene aggregation. Asphaltenes undergo dimer formation at 50 mg/L in toluene.[15] High-*Q* ultrasonic studies have recently established that asphaltenes have a critical nanoaggregate concentration (CNAC) at ∼150 mg/L in toluene.[16] Confirmation of these results has been obtained by NMR.[14] Furthermore, asphaltene nanoaggregates cluster at a concentration of several grams per liter in toluene.[17] Consequently, plotting the variable asphaltene aggregate weights versus the concentration and extrapolating to a low concentration does not guarantee molecular dispersion. In contrast, FCS measurements have been performed at asphaltene concentrations of 30 $\mu$g/L and confirm the low molecular weights of asphaltenes. LDI methods have routinely reported high molecular weights of asphaltenes;[18] however, these measurements most likely suffer from laser power and asphaltene concentration effects.[10] Gel permeation chromatography (GPC) has also been used to report high to ultrahigh molecular weights.[18] However, GPC studies of asphaltenes suffer from unknown aggregation effects and from the lack of standards to convert time to molecular weight for asphaltenes. In addition, the use of *N*-methyl pyrrolidinone in GPC studies[18] is known to cause asphaltene flocculation,[19] accounting for the reported putative ultrahigh molecular weights.[20]

With the resolution of asphaltene molecular weight, the next topic to address is asphaltene molecular structure. A variety of possible architectures have been proposed but most are ruled out by the small asphaltene molecular weights. A crucial concern in asphaltene molecular architecture is the size and shape of their fused aromatic ring (FAR) systems. Direct molecular imaging has been performed by scanning tunneling microscopy (STM), showing that asphaltene polycyclic aromatic hydrocarbons (PAHs) have 6−7 rings on average.[21] These results have been confirmed by high-resolution transmission electron microscopy (TEM).[22] Furthermore, the TEM studies show that coal asphaltenes have smaller PAH systems, as confirmed by three different techniques for measuring diffusion: TRFD,[5] FCS,[13] and TD.[11] With 6−7 rings in the PAH chromophore, ∼60% saturated carbon, and a molecular weight of 700 Da, a petroleum asphaltene molecule is limited to have only one PAH per molecule. This is exactly the conclusion from all TRFD measurements.[4−6] The "archipelago" model is refuted for the bulk of asphaltene; asphaltene molecules are shaped "like your hand" with a single aromatic core (palm), which has alkane substitution (fingers). The "like your hand" model is also called the "island" model and the "monomer" model of asphaltene molecular architecture. Asphaltenes are polydisperse; there will be some fraction of asphaltene molecules containing two fused rings, and much smaller asphaltene fraction containing three fused rings, etc.

The geometry of the aromatic rings in asphaltene molecules is of concern. Detailed molecular orbital (MO) calculations have been carried out on a vast number of PAHs to uncover systematics between PAH geometries and properties.[23,24] Linear catacondensed ring systems (where there are no bridgehead carbons shared by three rings) tend to be less stable and, therefore, are not expected in asphaltenes.[23,24] One might expect pericondensed PAHs in asphaltenes based on these stability arguments. $^{13}$C NMR measurements support this expectation.[25]

(10) Hortal, A. R.; Martinez-Haya, B.; Lobato, M. D.; Pedrosa, J. M.; Lago, S. On the determination of molecular weight distributions of asphaltenes and their aggregates in laser desorption ionization experiments. *J. Mass Spectrom.* **2006**, *41*, 960.

(11) Wargadalam, V. J.; Norinaga, K.; Iino, M. Size and shape of a coal asphaltene studied by viscosity and diffusion coefficient measurements. *Fuel* **2002**, *81*, 1403.

(12) Andrews, A. B.; Guerra, R. E.; Mullins, O. C.; Sen, P. N. Diffusivity of asphaltene molecules by fluorescence correlation spectroscopy. *J. Phys. Chem. A* **2006**, *110*, 8093.

(13) Guerra, R.; Andrews, A. B.; Ladavac, K.; Mullins, O. C.; Sen, P. N. Diffusivity of coal and petroleum asphaltene monomers by fluorescence correlation spectroscopy. *Energy Fuels*, manuscript to be submitted.

(14) Freed, D. E.; Lisitza, N. V.; Sen, P. N.; Song, Y.-Q. Molecular composition and dynamics of oils from diffusion measurements. In *Asphaltenes, Heavy Oils, and Petroleomics*; Mullins, O. C., Sheu, E. Y., Hammami, A., Marshall, A. G., Eds.; Springer: New York; Chapter 11, 2007.

(15) Goncalves, S.; Castillo, J.; Fernandez, A.; Hung, J. Absorbance and fluorescence spectroscopy on the aggregation behavior of asphaltene−toluene solutions. *Fuel* **2004**, *83*, 1823.

(16) Andreatta, G.; Bostrom, N.; Mullins, O. C. High-*Q* ultrasonic determination of the critical nanoaggregate concentration of asphaltenes and the critical micelle concentration of standard surfactants. *Langmuir* **2005**, *21*, 2728−2736.

(17) Yudin, I. K.; Anisimov, M. A. Dynamic light scattering monitoring of asphaltene aggregation in crude oils and hydrocarbon solutions. In *Asphaltenes, Heavy Oils, and Petroleomics*; Mullins, O. C., Sheu, E. Y., Hammami, A., Marshall, A. G., Eds.; Springer: New York; Chapter 18, 2007.

(18) Morgan, T. J.; Millan, M.; Behrouzi, M.; Herod, A. A.; Kandiyoti, R. On the limitations of UV-fluorescence spectroscopy in the detection of high-mass hydrocarbon molecules. *Energy Fuels* **2005**, *19*, 164.

(19) Badre, S.; Goncalves, C. C.; Norinaga, K.; Gustavson, G.; Mullins, O. C. Molecular size and weight of asphaltene and asphaltene solubility fractions from coals, crude oils and bitumen. *Fuel* **2006**, *85*, 1.

(20) Mullins, O. C. Rebuttal to comment by Professors Herod, Kandiyoti, and Bartle on molecular size and weight of asphaltene and asphaltene solubility fractions from coals, crude oils and bitumen by S. Badre, C. C. Goncalves, K. Norinaga, G. Gustavson and O. C. Mullins in *Fuel* **2006**, *85*, 1−11. Rebuttal published in *Fuel* **2007**, *86*, 309.

(21) Zajac, G. W.; Sethi, N. K.; Joseph, J. T. *Scanning Microsc.* **1994**, *8*, 463.

(22) Sharma, A.; Groenzin, H.; Tomita, A.; Mullins, O. C. Probing order in asphaltenes and aromatic ring systems by HRTEM. *Energy Fuels* **2002**, *16*, 490.

(23) Ruiz-Morales, Y. HOMO-LUMO Gap as an Index of Molecular Size and Structure for Polycyclic Aromatic Hydrocarbons (PAHs) and Asphaltenes: A Theoretical Study. I. *J. Phys. Chem. A* **2002**, *106*, 11283.

(24) Ruiz-Morales, Y. Molecular orbital calculations and optical transitions of PAHs and asphaltenes. In *Asphaltenes, Heavy Oils, and Petroleomics*; Mullins, O. C., Sheu, E. Y., Hammami, A., Marshall, A. G., Eds.; Springer: New York; Chapter 4, 2007.

(25) Scotti, R.; Montanari, L. NMR, IR, and EPR of asphaltenes. In *Structures and Dynamics of Asphaltenes*; Mullins, O.C., Sheu E. Y., Eds.; Plenum: New York, 1998.

Carbon X-ray Raman spectroscopy is a sensitive probe of carbon type in PAHs and clearly shows that the penultimate issue is that sextet carbon predominates in asphaltenes.[26,27] This designation will be explained shortly. Some catacondensed and many pericondensed structures have predominantly sextet carbon.

The PAHs in heavier crude oils and asphaltenes are known to be the source of their color.[28,29] Crude oil[30] and asphaltene[31] absorption spectra exhibit similar properties; for example, a single equation describes their electronic absorption edge.[30,31] In addition, their fluorescence emission spectra also exhibit similar properties.[32,33] For example, crude oils have been shown to obey the energy gap law,[33] which thereby governs crude oil quantum yields and controls the dynamics in energy transfer for chromophore collisional processes.[29,33]

In this study, we investigate one of the defining characteristics of asphaltenes, their color (or absorption spectra), as well as their fluorescence emission spectra. The quantitative comparison of asphaltene PAHs and the color that they impart is accomplished by a comparison of ubiquitous asphaltene spectra with predictions from MO calculations. Many (258) candidate PAHs are analyzed by MO calculations. Polydispersity is considered at the outset. Candidate PAHs are considered within the context of molecular stability and measured aromatic sextet carbon versus isolated double-bond carbon. The polydispersity of asphaltene ring systems is considered within optical spectral constraints of PAH population distributions. A consistent picture emerges; most probable asphaltene PAHs have 7 fused rings. Also, a comparison of the MO analysis with measured dispersion in the asphaltene diffusion constant strongly supports the "monomer" or "like your hand" description for the bulk of asphaltene molecules. The archipelago model is largely ruled out for the bulk of asphaltenes as being incompatible with what one observes with the eye, asphaltene color. Heteroatoms are mentioned and do not significantly modify the results herein.

## 2. Computational Methods

The geometry optimization of the PAH systems was done by performing force field (FF) based minimization using the energy minimization panel in Cerius2 version 4.6 and the COMPASS (condensed-phase optimized molecular potentials for atomistic simulation studies)[34,35] consistent FF, as provided in the Cerius2 package.[36] This type of minimization or geometry optimization is a molecular mechanics simulation, where the laws of classical physics are used to predict the structures and properties of molecules. The COMPASS FF has been tested and validated extensively against the experiment for many organic molecules. It is an *ab initio* FF that enables an accurate and simultaneous prediction of gas-phase properties (structural, conformational, vibrational, etc.) and condensed-phase properties (equation of state, cohesive energies, etc.) for a broad range of molecules and polymers.[35,36]

In previous studies,[23,24] we carried out the validation of the best combination of theoretical methods (optimization method/excited states calculation method and optimization method/single-point calculation method) that agree better with the experimental fluorescence emission data of PAHs. Thus, to find the best method for the geometry optimization of the structures, we tested three different methods: (1) using COMPASS FF-based minimization, (2) using the semiempirical PM3 method, and (3) using density functional theory and the B3LYP functional. The excited electronic states (including the frontier orbital $\pi-\pi^*$ transition) were calculated also using different methods: (1) the semiempirical electronic structure method ZINDO/S, (2) the semiempirical PM3 method, (3) a single-point calculation at the Hartree−Fock (HF) self-consistent field level, (4) a single-point calculation with the density functional theory (DFT) and the B3LYP functional, and (5) the time-dependent density functional theory (TD-DFT) to calculate the transition energy. We concluded that the best agreement between the theory and experiment is observed for the case of the FF/ZINDO calculations.[24] Thus, in the present study, the excited electronic states of the PAH systems were calculated using the ZINDO/S[37] method, as provided in the Gaussian 98 package,[38] and using the COMPASS FF geometry-optimized structures.

We have calculated the ultraviolet−visible (UV−vis) spectrum of PAH systems (some with N and S atoms in their structure) with 3−10 FARs. We have only calculated the UV−vis spectrum of neutral even-numbered PAHs with six-membered rings and not fived-membered rings (with carbon), that is, benzenoid-type PAHs (some with heteroatoms). The polycyclic aromatic compounds (PACs) contain in their structure one nitrogen atom in its pyridinic form or one sulfur atom. In the case of the nitrogen heteroatom, one carbon atom and its hydrogen in the PAH compounds are substituted by a nitrogen atom. The substitution is made in several places of the structure, and for each PAC, the UV−vis spectrum is calculated. For the case of PAC systems with a sulfur atom, the sulfur atom was located in a bay region to form a five-membered ring with thiophenic sulfur, which is the dominant form of aromatic sulfur in asphaltenes.[39]

The excited states of a total of 258 systems have been calculated. The total number of systems (PAHs and PACs) calculated for each FAR family is 3 FARs, 3 systems; 4 FARs, 5 systems; 5 FARs, 28 systems; 6 FARs, 27 systems; 7 FARs, 40 systems; 8 FARs, 36 systems; 9 FARs, 71 systems; and 10 FARs, 48 systems. The number of calculated spectra is equal to the number of systems for each FAR family. All of the calculated spectra for each FAR family were added up, and a population diagram versus the wavelength

(26) Bergmann, U.; Groenzin, H.; Mullins, O. C.; Glatzel, P.; Fetzer, J.; Cramer, S. P. Carbon K-edge X-ray Raman spectroscopy supports simple, yet powerful description of aromatic hydrocarbons and asphaltenes. *Chem. Phys. Lett.* **2003**, *369*, 184.

(27) Bergmann, U.; Mullins, O. C. Carbon X-ray Raman spectroscopy of PAHs and asphaltenes. In *Asphaltenes, Heavy Oils, and Petroleomics*; Mullins, O. C., Sheu, E. Y., Hammami, A., Marshall, A. G., Eds.; Springer: New York; Chapter 5, 2007.

(28) Mullins, O. C. Asphaltenes in crude oil: Absorbers and/or scatterers in the near-infrared region?. *Anal. Chem.* **1990**, *62*, 508.

(29) Mullins, O. C. Optical interrogation of aromatic moieties in crude oils and asphaltenes. In *Structures and Dynamics of Asphaltenes*; Mullins, O.C., Sheu E. Y., Eds.; Plenum Press: New York, 1998; Chapter 2.

(30) Mullins, O. C.; Mitra-Kirtley, S.; Zhu, Y. Electronic absorption edge of petroleum. *Appl. Spectrosc.* **1992**, *46*, 1405.

(31) Mullins, O. C.; Zhu, Y. First observation of the Urbach tail in a multicomponent organic system. *Appl. Spectrosc.* **1992**, *46*, 354.

(32) Downare, T. D.; Mullins, O. C. Visible and near-infrared fluorescence of crude oils. *Appl. Spectrosc.* **1995**, *49*, 754.

(33) Ralston, C. Y.; Wu, X.; Mullins, O. C. Quantum yields of crude oils. *Appl. Spectrosc.* **1996**, *50*, 1563.

(34) Sun, H.; Ren, P.; Fried, J. R. *Comput. Theor. Polym. Sci.* **1998**, *8*, 229.

(35) Sun, H. *J. Phys. Chem. B* **1998**, *102*, 7338.

(36) Molecular Simulation Incorporated. Cerius2 Modeling Environment, release 4.0; Molecular Simulations Incorporated: San Diego, CA, 1999.

(37) Zerner, M. C.; Correa de Mello, P.; Hehenberger, M. *Int. J. Quantum Chem.* **1982**, *21*, 251.

(38) Frisch, M. J.; Trucks, G. W.; Schlegel, H. B.; Scuseria, G. E.; Robb, M. A.; Cheeseman, J. R.; Zakrzewski, V. G.; Montgomery, J. A., Jr.; Stratmann, R. E.; Burant, J. C.; Dapprich, S.; Millam, J. M.; Daniels, A. D.; Kudin, K. N.; Strain, M. C.; Farkas, O.; Tomasi, J.; Barone, V.; Cossi, M.; Cammi, R.; Mennucci, B.; Pomelli, C.; Adamo, C.; Clifford, S.; Ochterski, J.; Petersson, G. A.; Ayala, P. Y.; Cui, Q.; Morokuma, K.; Malick, D. K.; Rabuck, A. D.; Raghavachari, K.; Foresman, J. B.; Cioslowski, J.; Ortiz, J. V.; Stefanov, B. B.; Liu, G.; Liashenko, A.; Piskorz, P.; Komaromi, I.; Gomperts, R.; Martin, R. L.; Fox, D. J.; Keith, T.; Al-Laham, M. A.; Peng, C. Y.; Nanayakkara, A.; Gonzalez, C.; Challacombe, M.; Gill, P. M. W.; Johnson, B. G.; Chen, W.; Wong, M. W.; Andres, J. L.; Head-Gordon, M.; Replogle, E. S.; Pople, J. A. Gaussian 98, revision A.7; Gaussian, Inc.: Pittsburgh, PA, 1998.

(39) Mullins, O. C. Sulfur and nitrogen xanes spectroscopy of carbonaceous materials. In *Asphaltenes, Fundamentals and Applications*; Sheu, E. Y., Mullins, O.C., Eds.; Plenum Press: New York, 1995; Chapter 2.

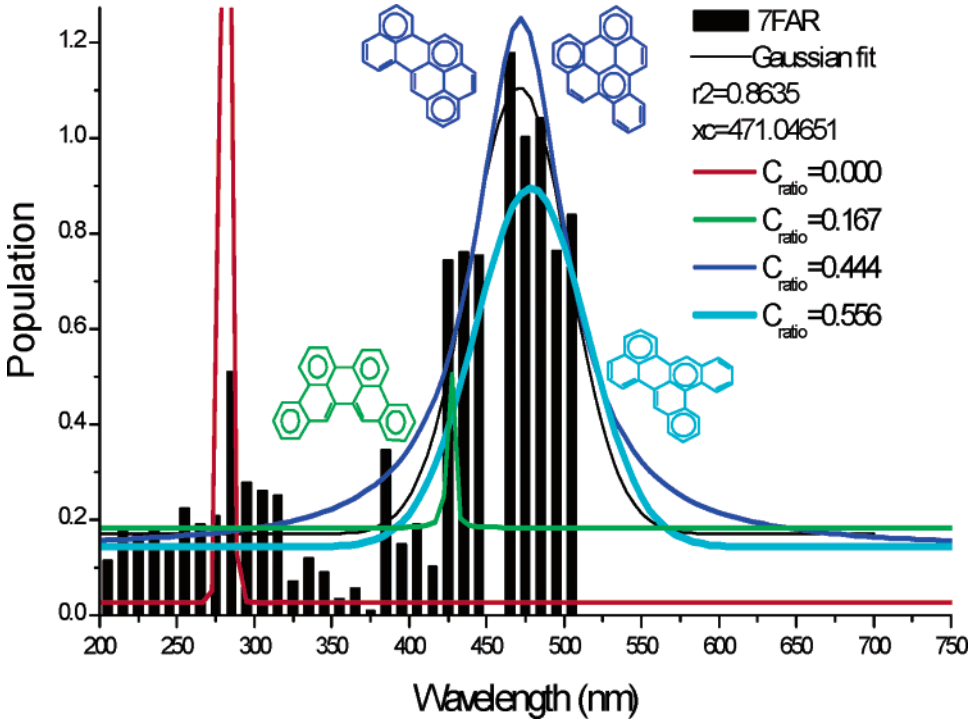


**Figure 1.** Results of the MO calculations for the 7 FAR PAHs. A total of 40 7 FAR PAHs were analyzed, and a few of the corresponding structures are shown in the figure. The bar chart represents the strength of electronic transitions in the spectral bands for these PAHs. All PAH transitions within a spectral range added to the height of the bar. Resulting spectra are shown.

was obtained. The population is the sum of the calculated UV−vis intensity, for all of the compounds, that fall in a given wavelength range, divided by the number of occurrences that fall in that given wavelength range. We chose wavelength ranges or regions of 10nm: 200−209nm, 210-219nm, 220−229 nm, and so on. Other means of normalization did not impact the data significantly.

For example, the graph of 7 FAR considers the calculated UV−vis spectra of 40 compounds. There are many more 7 FAR PAH compounds, but we only calculated 40. Only 33 compounds show intensity in the region of 280−289 nm, and there are a total of 62 entries or resonances, in that region, for these 33 compounds. The sum of all of the intensities for the 62 entries is 31.5987. Therefore, the population in the 280−289 wavelength region is equal to 31.5987 divided by 62 = 0.5096. As shown in Figure 1, in the 7 FAR graph, there is a black bar in the region of 280−289 (centered in 285 nm) with a height of 0.5096. In the same way, all of the black bars, along the wavelength axis, are obtained. The total population, shown by black bars in the calculated results, is used to obtain the best Gaussian fit for all of the calculated 7 FAR family (black curve). The black curve in Figure 1 represents the Urbach tail for each FAR family.

Once the Urbach tail for each FAR family was obtained, we obtained the best Gaussian fit that represents the population versus the wavelength for the different systems that present the same C ratio (carbon ratio curves), that is, the ratio of carbon atoms (C ratio) in isolated double bonds versus aromatic sextet rings.[26,27] The procedure changes slightly to obtain the C ratio curves. In continuation with the example of the 7 FAR family, only four compounds, of the 40 analyzed compounds, have a carbon ratio = 0. Thus, the red curve (in the 7 FAR graph), which corresponds to a C ratio = 0.00, represents the best Gaussian fit for a population, constructed in the same way explained above, that only contains the intensities of four compounds and their occurrences. In general, for the case of the higher carbon ratios, the population of the graph that contains all of the compounds with the same carbon ratio is not too different to the populations presented in the general graph that contains the 40 systems. Thus, the corresponding peaks for the higher C ratios are not that persistent.

The compounds with a low carbon ratio have a high number of resonant sextets in the structure (almost full resonant such as triphenylene). There are a few of these compounds in each FAR family. Thus, there persists a short wavelength peak for nearly fully sextet compounds independent of the number of rings.

## 3. Experimental Section

Asphaltenes prepared by *n*-heptane precipitation were used throughout. *n*-Heptane was added in a ratio of 40 $cm^3$/g of crude oil to flocculate the asphaltenes. The solution was stirred and kept in the dark. After 24 h, the solution was filtered. The resulting precipitate was washed with hot *n*-heptane. The collected asphaltenes were dissolved in a minimum amount of toluene and then precipitated again using *n*-heptane in the same 40 $cm^3$/g ratio. We have never observed any effect of the second precipitation process on any of our data.

All optical absorption spectra were collected using a Cary 5 UV−vis−near-infrared (NIR) spectrometer. Typically, 2 mm path lengths were used. This matches the path length of our downhole spectrometer used to obtain vis−NIR spectra of crude oils in situ in oil wells.[40] Fluorescence measurements were made on a PTI C-72 and A-720 fluorescence spectrometer using a 75 W Xe compact arc lamp source.

**The Clar Representation of PAHs.** Our purpose here is to report simple heuristics which result from the detailed MO calculations. Fortunately, these simple heuristics are generally accessible and do not require significant knowledge of MO calculation methods. Furthermore, these simple ideas are dominant in asphaltene PAH identity. However, these simplifying concepts are not part of standard chemistry curricula. We provide a brief overview.

As taught in Freshman chemistry, the alternating double and single bonds of benzene are in fact equivalent in terms of bond length, electron density, etc. and are often represented by embedding a circle in the benzene ring (cf. Figure 2). Of course, one can represent the $\pi$ electrons of benzene by the two contributing Kekulé structures (cf. Figure 2). These Kekulé structures are understood

(40) Fujisawa, G.; Mullins, O. C. Downhole fluid analysis and acquisition of live crude oil samples. In *Asphaltenes, Heavy Oils, and Petroleomics*; Mullins, O. C., Sheu, E. Y., Hammami, A., Marshall, A. G., Eds.; Springer: New York; Chapter 22, 2007.

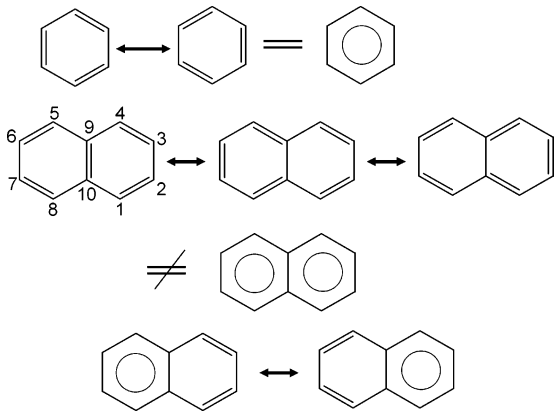


**Figure 2.** Clar representation of PAHs provides a more accurate description of the electron density. The stability of PAHs is graphically assessed by noting the fraction of aromatic sextet carbon versus isolated double-bond carbon. Within the Clar representation, two adjacent hexagons cannot both be represented by hexagons with embedded circles, by far the most popular but less accurate way of representing PAHs. That is, only one of the two adjacent rings gets the double bond for its aromatic sextet.

to be simultaneously contributing to the benzene electron wavefunctions as opposed to some sort of alternating electron density. However, the Kekulé representation is less convenient because one now has twice the number of structures to consider, each with nonequivalent representations of equivalent bonds. Because the embedded circle is viewed as equivalent to the resonant Kekulé structures, the shorthand representation of the embedded circle to represent benzene is by far the more popular.

It is natural to extend this embedded circle representation to naphthalene. Thus, one might represent the alternating double and single bonds of naphthalene with two embedded circles. Analogous to benzene, one can represent naphthalene with three Kekulé structures (cf. Figure 2). Again, the Kekulé structures are not popular because of the proliferation of structures to be considered. For naphthalene, the embedded circle representation is far more popular. For larger ring systems, it is nearly uniform in the literature that the embedded circle is used to represent $\pi$ electrons in large PAHs and in candidate asphaltene PAHs. The implication of the embedded circle representation of electron density is that the zeroth-order electron distribution in PAHs is equal for each carbon. Of course, one expects that in reality there would be some less symmetric distribution. Nevertheless the zeroth-order representation is thought to be sufficiently conceptual as a guide to PAH electron density. After all, the embedded circle representation works well for benzene; why not use this for other PAHs? Keeping track of a large number of Kekulé structures is not really a viable alternative.

In fact, the embedded circle representation breaks down for naphthalene, and it misses some of the most important attributes of larger PAHs. Furthermore, there is a very simple representation that can be used in its place, the Clar representation, which conveys the electron density of PAHs and gives a strong indication about their stability.[41] First, we consider naphthalene. The embedded circle representation of naphthalene would indicate that all carbon−carbon bonds are the same bond order and, thus, the same length. In fact, in naphthalene, there are three different carbon−carbon bond lengths. The C1−C2 bond is the shortest; the C9−C10 bond is intermediate; and the C10−C1 bond is the longest. Obviously, this ordering of bond lengths does not follow from the embedded circle representation. Fortunately, a better representation of PAHs can be applied quite simply.

We now consider the Clar representation of $\pi$ electron density in aromatic rings.[41] A central feature of the Clar representation is the method of treating double bonds, which are shared between two rings. Consider a Kekulé structure with a double bond in the CC bond shared by two rings such as the C9−C10 bond in naphthalene (cf. Figure 2). Instead of treating this double bond as shared between two rings, in the Clar representation, this double bond is assigned to one of the two rings. In naphthalene, with this assignment, we now have one ring with three double bonds and the other ring with two double bonds. The ring with three double bonds is viewed as an aromatic sextet, with all six CC bonds being equivalent. However, the other ring with only two double bonds is viewed as containing two isolated double bonds and with differing bond orders in this ring.

We now reconsider naphthalene within the Clar representation (a similar analysis follows from analyzing the Kekulé structures). The bottom of Figure 2 shows two Clar structures of naphthalene. Naphthalene is seen to have one aromatic sextet and two isolated double bonds. The order of bond lengths can now be obtained. The shortest bond is C1−C2 (and the other equivalents) because this bond is on the order of 1.5 in one Clar structure and on the order of 2 in the other, with the average being a 1.75 bond order. The C9−C10 bond is on the order of 1.5 in both Clar structures. The C10−C1 bond is on the order of 1 in one Clar structure and on the order of 1.5 in the other, giving an order of 1.25. Thus, the Clar representation gives the ordering of bond lengths in naphthalene. One considers both Kekulé structures in the Clar representation; the two rings of naphthalene are equivalent. Analyzing other PAHs such as coronene quickly reveals the value of the Clar representation. Again, both Kekulé structures of the Clar representation must be consider; coronene has $D_{6h}$ symmetry.

In addition to providing the order of bond lengths, the Clar representation immediately provides an approximate idea of the stability of any PAH. Here is another important manifestation where the Clar representation is superior to the standard Kekulé representation. PAHs with a higher fraction of aromatic sextet carbon are more stable, while PAHs with a higher fraction of isolated double-bond carbon are less stable. Almost always, for any PAH, if different Clar representations are possible, the one with the great number of aromatic sextet carbon is preferred. The Y-rule has been developed to assign the location of the sextets.[23,24] In addition, the PAHs that are less stable have lower energy electronic transitions. Consider two four-ring PAHs; tetracene (one sextet ring) is colored and unstable with respect to degradation, while triphylene (three sextet rings) is colorless and stable. For PAHs, the underlying stability question is the ratio of aromatic sextet carbon to isolated double-bond carbon. Both tetracene and triphenylene are catacondensed; it is the aromatic sextet carbon and not the cata- versus pericondensation that determines stability.

Moreover, the Clar representation has been verified by carbon X-ray Raman spectroscopy (XRRS). In accordance with known spectral principles in X-ray spectroscopy,[39] increasing the isolated double-bond carbon fraction in PAHs results in an increase in the $1s-\pi^*$ resonant line width.[26,27] When asphaltene carbon was analyzed, XRRS showed that aromatic sextet carbon dominates. It is not pericondensation that tends to be favored in asphaltenes for some unknown geometric reason; it is molecular stability.[23,24] After all, the asphaltenes had to survive geologic time at elevated temperatures. Pericyclic PAHs tend to have a greater fraction of aromatic sextet carbon compared to catacondensed PAHs; asphaltenes may have pericyclic contributions.[24,26,27] Because there are very few purely sextet systems, from an entropy point of view, asphaltene PAHs should be mostly but not solely sextet carbon. XRRS studies have shown that there is roughly one isolated double bond per sextet ring in asphaltene PAHs. In this paper, we will represent asphaltene PAHs with only one of the possible Kekulé structures in the Clar representation.

## 3. Results and Discussion

**Asphaltene Spectral Properties.** Figure 3 shows the optical absorption edge of many crude oils from light to heavy.[30] In these spectra, there is no optical light scattering;[28] therefore, the optical density is equal to absorption. Figure 4 replots these

(41) Clar, E. *The Aromatic Sextet*; Wiley: London, U.K., 1972.

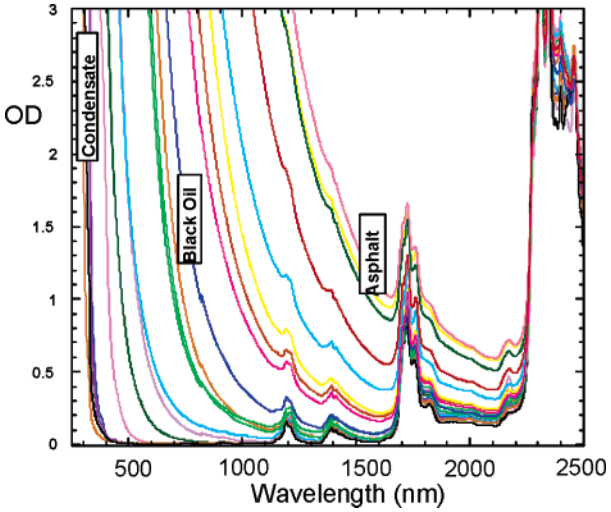


**Figure 3.** Electronic absorption edge of many crude oils; there is a large variation in the location of the spectral edge determined by the heavy end content of the crude oil. Several vibrational overtones are evident as isolated peaks.

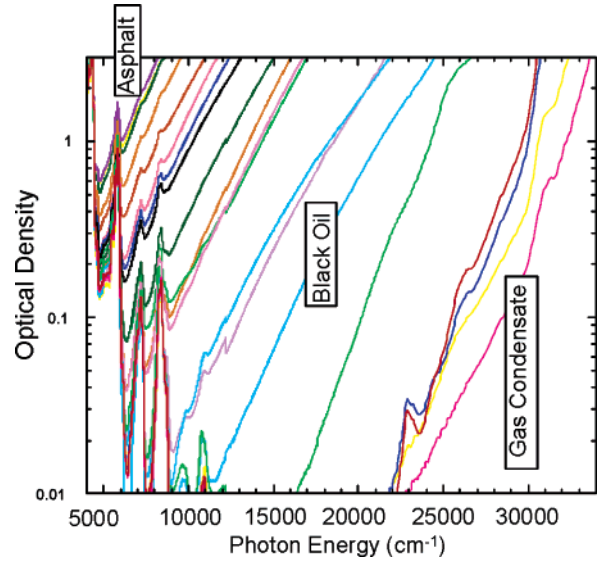


**Figure 4.** When the data of Figure 3 are plotted on a log−lin plot versus photon energy, one obtains the surprising result that all crude oils exhibit the same, linear slope of the absorption edge. As explained in the text, this is reminiscent of the Urbach tail first noted in solid-state physics.

spectra, where optical absorption is plotted on a log scale versus photon energy on a linear scale (a log−lin plot). The uniformity of the slope in Figure 4, independent of crude oil type or spectral location of the electronic absorption edge, is evident. Vibrational overtones are also evident in Figures 3 and 4 but are not of concern here. Asphaltenes show similar traits in their electronic absorption edge as shown in Figure 5. As has been pointed out,[29−31] the similarity of the slope in these spectra is determined by the population distribution of chromophores, which absorb light in the electronic spectral edge of a given crude oil or asphaltene. A linear slope on such a log−lin plot was first observed in silver halides by Urbach.[42] He showed that semiconductors do not have an infinitely sharp electronic absorption edge because of the thermal excitation of absorber cites; the slope of the Urbach tail is $kT$ ($k$ is Boltzmann's

(42) Urbach, F. *Phys. Rev.* **1953**, *92*, 1324.

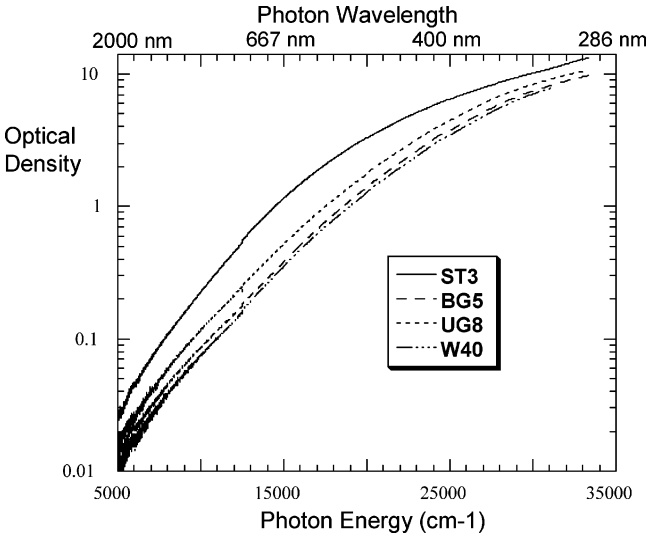


**Figure 5.** Asphaltenes exhibit the Urbach tail, the same linear slope in the electronic absorption edge. The exponential decrease in absorption for asphaltenes starts at ~650 nm and goes to 2 $\mu$m, corresponding to an exponential decline in corresponding asphaltene PAHs that absorb at progressively longer wavelengths.

constant, and $T$ is temperature). For crude oils and asphaltenes, the corresponding slope is $10kT$. Crude oils are not colored as a result of the presence of hot benzene but rather because of the thermal production of larger, spectrally red chromophores from smaller, spectrally blue chromophores. This picture is consistent with the expected finding that larger aromatics tend to be redder in spectral properties (both absorption and emission).[22,23] The more subtle but crucial issue of the effect of PAH geometry on spectral properties was also sorted out[22−24] largely within the Clar representation.

Examination of Figure 5 shows that the Urbach tail (the linear section of the plot) starts roughly at a wavelength of ~650 nm and extends to a wavelength of 2 $\mu$m, where the optical density drops to very low values. Thus, those asphaltene chromphores responsible for this increasing red-shifted absorption are present in exponentially decreasing concentrations. The presumption is that the oscillator (or optical absorption) strengths are roughly comparable for asphaltene chromophores throughout this range. This absorption edge or slope establishes limits for the largest possible chromophores in asphaltenes.

In addition, the lack of UV fluorescence in asphaltenes has been investigated.[43] Figure 6 shows that asphaltene fluorescence emission spectra lack emission from single-ring and two-ring systems. In addition, asphaltenes have little emission in the range where three fused ring PAHs fluoresce. If these small, blue-emitting chromophores were present in asphaltenes but were undergoing radiationless transitions, then the fluorescence lifetimes would be reduced substantially.[44] The fact that UV-emission fluorescence lifetimes for maltenes and asphaltenes are comparable suggests that there is no significant radiationless transition for blue-emitting asphaltene chromophores. The lack of UV emission from asphaltenes is due to the lack of smaller PAHs. Ultrahigh-resolution mass spectroscopy shows that the average number of aromatic rings in asphaltenes is 7[7] and thus corroborates conclusions that small ring systems are absent.

(43) Ralston, C. Y.; Mitra-Kirtley, S.; Mullins, O. C. Small population of one to three fused-ring aromatic molecules in asphaltenes. *Energy Fuels* **1996**, *10*, 623.

(44) Wang, X.; Mullins, O. C. Fluorescence lifetime studies of crude oils. *Appl. Spectrosc.* **1994**, *48*, 977.

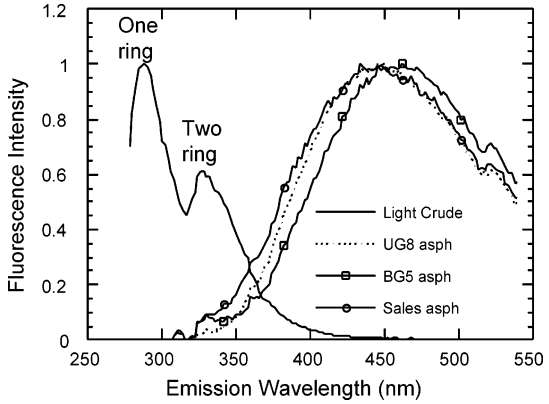


**Figure 6.** Emission spectra of asphaltenes show a maximum around 450 nm, providing a constraint on the identity of proposed asphaltene PAHs. The lack of fluorescence emission for one-, two-, and to some extent, three-ring PAHs for asphaltenes indicates a lack of these ring systems in asphaltenes.

Molecules with only a single aromatic ring will tend to be soluble in *n*-heptane and thus not be part of the asphaltene fraction, likewise for two-ring alkyl aromatics.

With the spectral maximum and minimum determined, we now address the bulk of the asphaltene fluorophores. In particular, we are interested in relating the calculated and measured highest occupied molecular orbital to lowest unoccupied molecular orbital (HOMO−LUMO) transition energy. The measured HOMO−LUMO is given by the fluorescence emission spectrum. Optical absorption includes excitation to the lowest energy transitions as well as to higher excited states. In a polydisperse sample, such as asphaltenes, the optical absorption at a particular wavelength includes excitation of the HOMO−LUMO of certain chromophores as well as excitation of higher excited states of lower energy chromophores. Only at the absorption edge can this process be ruled out because of the rapidly declining population of larger, redder chromophores. However, with rare exception, fluorescence emission of PAHs (in dilute solution) consists of fluorescence emission from the lowest lying excited state.[45] Thus, in fluorescence emission for asphaltenes, one obtains a spectral map of the HOMO−LUMO profiles of the asphaltene PAHs.

Figure 6 shows a standard fluorescence emission spectrum of an asphaltene. This spectrum is very typical for asphaltenes, exhibiting a maximum emission at ∼450 nm. As a very rough approximation, we use this emission spectrum as a guide to the population distribution of asphaltene fluorophores. We note the limitation that the quantum yield of these fluorophores does vary across the UV, vis, and NIR.[33] Nevertheless, this fluorescence maximum does fit very comfortably between the long wavelength constraint established by optical absorption and necessarily is to the red of the fluorescence minimum in the UV, establishing the short wavelength limit. These constraints can be used in conjunction with MO calculations to identify candidate asphaltene PAHs. However, one more critical issue of asphaltene PAHs must be considered first.

Within the Clar representation, PAHs with a large fraction of sextet carbon are much more stable and spectrally blue-shifted.[22,23] Corresponding PAHs with a large fraction of isolated double-bond carbon are unstable and red-shifted.[22,23] XRRS spectroscopy has utilized the 1s−$\pi$* transition of a large number of PAHs and asphaltenes. These studies show that the PAHs of asphaltenes are predominantly sextet carbon.[26,27] This observation is in accordance with the stability that asphaltenes have exhibited by surviving for geologic time at elevated temperatures in oil reservoirs. The exact ratio of carbon atoms in isolated double bonds to those in aromatic sextets is a bit difficult to determine from XRRS but is on the order of 1:3 for isolated double-bond carbon/sextet carbon for the bulk asphaltene sample.

**Summary of MO Calculations on PAHs.** Figure 7 shows the results of the MO calculations on a large number of PAHs. This figure lists the spectral location of the allowed electronic transitions of particular PAHs that have been studied here within the wavelength range shown here. The calculation presumes no solvent. The presence of a solvent is expected to blue-shift excitation and red-shift fluorescence emission by roughly 25 nm. There are many important conclusions to note. Figure 7 shows the overall trend that PAHs with greater numbers of fused ring systems show red-shifted spectra. Furthermore, for a given fused ring number, PAHs that have a greater fraction of sextet carbon exhibited blue-shifted spectra. PAHs that are fully sextet or almost fully sextet exhibit HOMO−LUMO transitions in the UV. It is true that subtle changes in ring geometry can have dramatic spectral consequences. For example, ovalene (10 FARs conceptually made by fusing phenanthrene onto coronene) has a UV HOMO−LUMO (310 nm), while a less symmetric compound with 10 FARs conceptually made by moving one of ovalenes rings has an orange HOMO−LUMO (575 nm) and only a slightly lower ratio of sextet carbon. Nevertheless, the two overriding factors controlling PAH spectral properties are the fused ring number and fraction of sextet carbon.

**Quantitative Interpretation via the MO Calculation of Asphaltene Spectra.** Because asphaltenes do not exhibit much UV fluorescence, the implication is clear: asphaltene PAHs are mostly not fully sextet. This finding is supported in two ways. First, the XRRS results clearly show a strong contrast between fully sextet PAHs and asphaltene PAHs.[26,27] Second, it has been established repeatedly by measuring asphaltene diffusion constants using TRFD that the blue-emitting fluorophores are the smallest asphaltene molecules.[4−6,46] However, the fully sextet PAHs are not small in size. There are PAHs with 6-, 8-, and 10-fused rings that are mostly or entirely sextet carbon and that have HOMO−LUMO transitions in the UV. Such PAHs would give large diffusion constants and not the measured small diffusion constants for UV-emitting asphaltene PAHs. Thus, we conclude three lines of investigation: spectral analysis with the MO calculation, XRRS results, and TRFD results; all show that asphaltene PAHs are not fully sextet.

Figure 7 shows that many PAHs with 6, 7, and 8 FARs have electronic transitions in the range where asphaltenes show fluorescence maxima in the 450 nm range. Most of these compounds are close to a isolated double-bond (IDB)/sextet carbon ratio of 0.3333. Thus, the spectral analysis using the MO calculation supports the perspective that petroleum asphaltenes possess a dominance of PAHs with 6−8 FARs. Direct molecular imaging using STM concludes exactly the same result.[21] In this STM study, atomic imaging enabled the ability to show the particular rings. In addition, a histogram of the PAH ring sizes showed a maximum at ∼11 Å. Direct molecular imaging of aromatic sheets of asphaltenes using HRTEM also concludes the same result.[22]

In the Urbach tail range at ∼650 nm, Figure 7 shows that, of ring systems analyzed here, only 9- and 10-FAR systems contribute. Because of the rapidly diminishing optical absorption

(45) Turro, N. J. *Modern Molecular Photochemistry*; The Benjamin/Cummings Pub. Co.: Menlo Park, CA, 1978.

(46) Groenzin, H.; Mullins, O. C.; Eser, S.; Mathews, J.; Yang, M.-G.; Jones, D. Asphaltene molecular size for solubility subfractions obtained by fluorescence depolarization. *Energy Fuels* **2003**, *17*, 498.

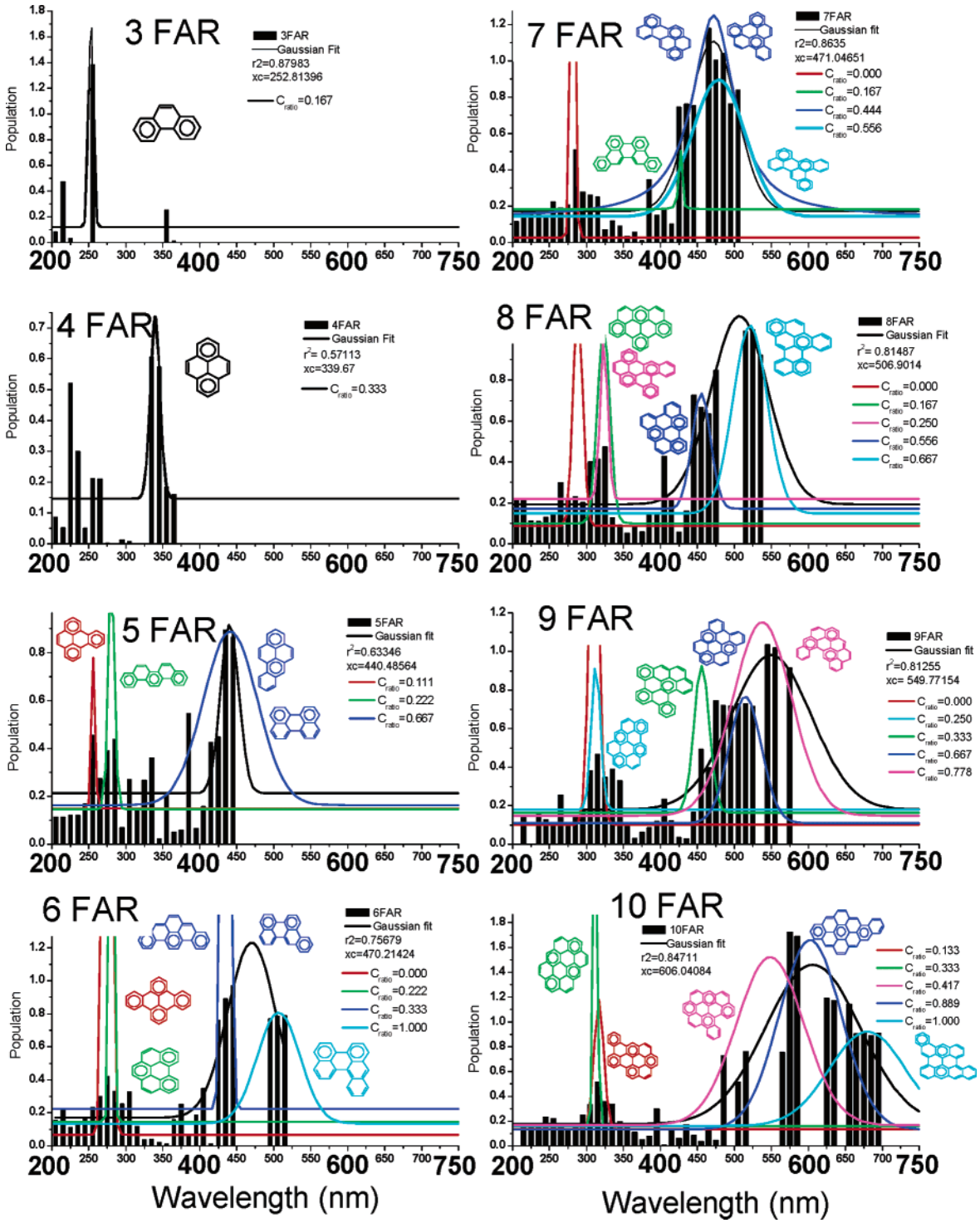


**Figure 7.** Results of analyzing 258 PAHs with numbers of FARs varying from 3 to 10. The spectral locations of the electronic transitions are recorded with the bar chart (cf. Figure 1). A comparison of these MO calculations versus asphaltene spectra (Figure 6) shows that PAHs with 6−8 FARs are dominant in asphaltenes. The structures of a few ring systems and their spectral location are shown. Asphaltenes have been shown to possess roughly one sextet ring per isolated double bond,[26,27] in accordance with the molecular stability assessment;[23,24] therefore, those ring systems were emphasized. Note the increase in the wavelength for the (1) increasing FAR number and (2) decreasing sextet ratio (cf. Figure 2).

in this spectral range, we conclude that asphaltenes with 10-fused or more aromatic rings are not common. We note that we arbitrarily terminated the investigation of PAHs above 10 FARs. We are confident that all trends already established in Figure 7 for PAHs would continue; this will be investigated in the near future. Indeed, TRFD studies have established that the spectrally reddest (longest wavelength) asphaltene molecules are the largest, thus, consistent with this MO analysis.[4−6,46] Furthermore, these large asphaltene molecules are also the least soluble in toluene−*n*-heptane mixtures.[46] The resulting conclusion is that the asphaltene molecules in the high-molecular-weight tail of the distribution are comprised of the largest, spectrally reddest shifted PAHs. The large mass tail of asphaltenes might have much bigger PAHs.

**"Monomeric" Asphaltene Molecular Structure versus the "Archipelago" Model.** Various models have been proposed for the asphaltene molecular structure. The "monomeric" model, which equals the "like your hand" model for asphaltene

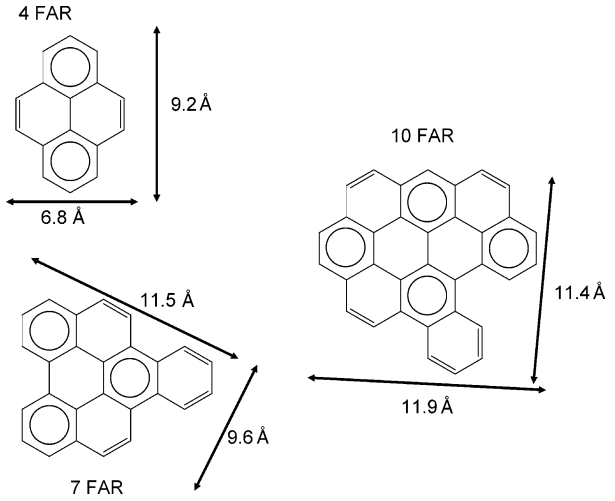


**Figure 8.** Sizes of a few PAHs of differing FAR number.

molecules, comprises molecules with a single PAH ring system (the palm) surrounded by alkane substitution (the fingers). The archipelago model would covalently link several of these monomeric units with alkane chains and sulfide bridges, etc. First, the proposed structure must fit within the molecular weight of asphaltenes. Four molecular diffusion measurements of asphaltenes are in accord and show that asphaltene molecular weights are fairly small, with a mean around 750 Da. These techniques are time-resolved fluorescence depolarization,[4−6,46] Taylor dispersion,[11] fluorescence correlation spectroscopy,[12,13] and NMR.[14] All mass spectral ionization techniques are consistent and reveal that asphaltene molecular weights are small, including field ionization,[3] electrospray ionization,[7] atmospheric pressure photoionization,[8] and atmospheric pressure chemical ionization.[8,9] Added to this formidable array, it has now been established that laser desorption ionization yields results in accordance with all diffusion and all other ionization methods for mass spectrometry when performed with a low laser power and low asphaltene concentration.[10] This important publication[10] not only confirms the small asphaltene molecular weights but also shows how LDMS and MALDI results published elsewhere[18] suffer huge artifact problems.

For asphaltene molecular weights averaging 750 Da and for the PAHs established herein, only one PAH can fit in an asphaltene molecule (for the bulk of the asphaltene molecular population). To put this more colloquially, petroleum asphaltenes are black. We show quantitatively that this coloration necessitates PAHs of roughly 7-fused rings of requisite sextet ratio. Given that petroleum asphaltenes are roughly 60% alkane carbon, the resulting structure can contain only one FAR system. The fact that the biggest asphaltene molecules are the reddest shifted[4−6,46] and, as shown in Figure 7, the reddest shifted PAHs are the largest (e.g., 10-fused rings), then it follows there is only one ring system per molecule. In short, the monomeric model of asphaltenes is supported; the archipelago model is refuted for the bulk of asphaltenes. What remains to be investigated is whether the largest asphaltene molecules in the high mass tail still consist primarily of a single, large PAH core with peripheral alkanes.

Figure 8 shows the molecular size of several of the PAH ring systems that the analysis herein purports are among good candidate structures for asphaltenes. These sizes compare favorably with the sizes obtained via direct molecular imaging. An STM of asphaltenes study with its atomic imaging capability found the most probable ring size to be 11 Å.[21] An HRTEM

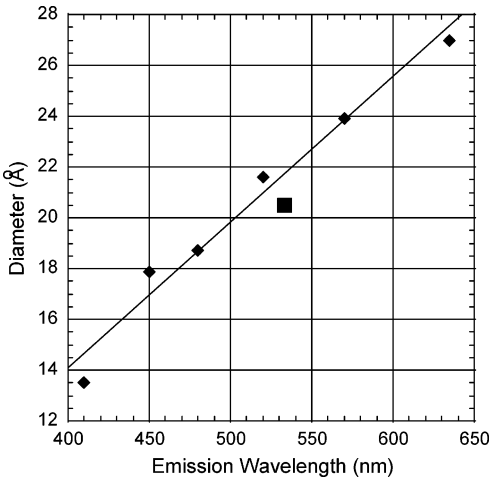


**Figure 9.** Measured hydrodynamic diameter (long axis, oblate spheroid) of asphaltene molecules versus fluorescence emission wavelength.[4] A solar dye is also shown (■), which has a 7 FAR PAH and ∼50% alkane carbon. The alkane carbon fraction of asphaltene and solar dye yields a hydrodynamic twice the physical size of the PAH core. Evidently, a longer emission wavelength corresponds to larger PAH systems in accordance with Figure 7.

study of asphaltenes, with its aromatic sheet imaging capability, found asphaltenes to be ∼10 Å.[22] Figure 9 shows the measured molecular sizes of asphaltenes versus the fluorescence emission wavelength as determined by TRFD.[4] The asphaltene molecules are roughly twice the size of the fused aromatic cores shown in Figure 8. This also applies for "solar dye", which has a 7 FAR PAH. Just as with the asphaltenes, the measured size of the solar dye molecules is twice the size of the aromatic core. For both asphaltenes and solar dye, only 40 or 50%, respectively, of the carbon is aromatic; the rest is saturated. Doubling the carbon content beyond that in the aromatic core apparently doubles the molecular hydrodynamic size. A shorter emission wavelength is correlated with a smaller molecular size. This is expected (cf. Figures 7 and 8) only if there is a single PAH per asphaltene molecule. Thus, a comparison of asphaltene PAH spectra and measured asphaltene molecular size at different wavelengths supports the "monomeric" model of asphaltenes.

Finally, we note that coal asphaltenes are much smaller than petroleum asphaltenes.[5,6,11,13,47] A similar analysis needs to be performed for coal asphaltenes. We anticipate that coal asphaltenes will be shown to possess smaller fused ring systems than petroleum asphaltenes.

## 4. Conclusions

MO calculations particularly of PAHs have a long and rich history. Here, we use MO calculations to interpret quantitatively the ubiquitous and highly constraining optical absorption and emission spectra of petroleum asphaltenes. This study shows that two fundamental parameters largely control PAH optical properties: (1) the number of fused rings and (2) the ratio of isolated double-bond carbon/sextet carbon. It has previously been established that asphaltenes are largely but not entirely sextet carbon.[23] Several fundamental conclusions are drawn regarding asphaltenes. Petroleum asphaltenes consist of PAHs mostly with 6−8 FARs. Asphaltene molecules span a range having appreciable molecular populations with ∼4−10 fused aromatic rings. Given the small molecular weights of petroleum

(47) Buenrostro-Gonzalez, E.; Groenzin, H.; Lira-Galeana, C.; Mullins, O. C. The overriding chemical principles that define asphaltenes. *Energy Fuels* **2001**, *15*, 972.

asphaltenes, there can only be one PAH per asphaltene molecule on average. This "monomeric" molecular model for asphaltenes is consistent with MO calculations coupled with the measured wavelength dependence of the asphaltene molecular size. Blue-emitting asphaltene molecules are small and possess a single small PAH; red-emitting asphaltene molecules are big with a single large PAH. The "monomeric" model, which equals the "like your hand" model of asphaltenes, is supported; the archipelago model is refuted for the bulk of asphaltenes.

**Acknowledgment.** The theoretical research in this work has been supported under projects D.00345 and D.00406 of the Instituto Mexicano del Petróleo (IMP).

EF060250M